# Chapter 5 Eroded Critical Zone Carbon and Where to Find It: Examples from the IML-CZO



Neal Blair D, John M. Hayes, David Grimley D, and Alison M. Anders D

#### 5.1 Introduction

Humans have accelerated the erosion of the Critical Zone (CZ) by 3- to 5-fold, and in doing so have perturbed nearly half of the land surface globally (Hooke 2000; Wilkinson and McElroy 2007; Amundson et al. 2015). Most of the disturbance has been driven by deforestation and tillage and these activities often lead to substantial local losses of soil organic C via oxidation and erosion (OC; Lal 2003; Papanicolaou et al. 2015).

Early C-budgets suggested that the oxidative loss represented a net gain of CO<sub>2</sub> to the atmosphere, thereby contributing to the already disruptive burden from fossil fuel combustion (Lal 2003). Subsequently, processes were identified that not only mitigate the CO<sub>2</sub> addition but could possibly tip the soil erosion C-budget into being a net sink of CO<sub>2</sub> (Harden et al. 1999; Berhe et al. 2007; Doetterl et al. 2016; Wang et al. 2017). The loading of OC onto freshly exposed, but OC-poor subsurface soils, termed dynamic replacement, partially reverses the C-flux to the atmosphere (Harden et al. 1999). If coupled with the downslope accumulation and sequestration of the eroded portion of the soil OC, dynamic replacement could facilitate a net removal of CO<sub>2</sub> from the atmosphere (Berhe et al. 2007; Doetterl et al. 2016). The nature of the

N. Blair (⋈) · J. M. Hayes

Departments of Civil and Environmental Engineering, and Earth and Planetary Sciences, Northwestern University, Evanston, IL 60208, USA

e-mail: n-blair@northwestern.edu

D. Grimley

Illinois State Geological Survey, Prairie Research Institute, University of Illinois, Champaign, IL 61820, USA

e-mail: dgrimley@illinois.edu

A. M. Anders

Department of Geology, University of Illinois at Urbana Champaign, Urbana, IL 61801, USA e-mail: amanders@illinois.edu

© Springer Nature Switzerland AG 2022

Zone Science, https://doi.org/10.1007/978-3-030-95921-0\_5

A. S. Wymore et al. (eds.), *Biogeochemistry of the Critical Zone*, Advances in Critical

depositional environment that receives the eroded materials is critical however, and this has not been well-considered. Highly dynamic settings, such as large river deltas (e.g., those of the Mississippi and Amazon Rivers), have been termed C-incinerators because of their ability to oxidize terrestrial OC (Aller and Blair 2006; Blair and Aller 2012). Approximately 70% of soil OC delivered to those locations will contribute to the atmospheric source (Blair and Aller 2012). In contrast, rapidly accumulating, relatively quiescent settings, such as lakes, will preserve more of the soil OC (Smith et al. 2001; Blair and Aller 2012; Blair et al. 2018). Vegetative inputs to depositional soils, and algal OC in aquatic systems, further tip the entire landscape budget into being a net C-sink. Where the soil OC goes after erosion thus becomes an important consideration when attempting to balance the C-ledger.

The disruption of the CZ root-soil aggregate fabric by the removal of vegetation and/or soil mixing increases the vulnerability of OC to oxidation and erosion (Doetterl et al. 2016). The eroded material is redistributed across the landscape to depositional sites broadly characterized as (1) colluvium and alluvium deposited at the base of hillslopes or in closed depressions, (2) sediments transported fluvially and deposited in channels or on floodplains as alluvium, and (3) sediments trapped by lakes and reservoirs (Meade et al. 1990; Stallard 1998). Between about 50 to 95% of eroded C is redeposited within some watersheds (Van Oost et al. 2007). Less than 10% of the eroded soil and its C is thought to escape the continental land mass to be exported to the ocean (Meade et al. 1990; Stallard 1998). However, this estimate is highly influenced by budgets done on river systems that have extensive low gradient sections with a large storage capacity (Milliman and Meade 1983). Much higher export efficiencies are expected from small, high-relief watersheds, such as those lining the Pacific Rim (Milliman and Syvitski 1992).

Intuitively, depositional fluxes should attenuate with distance from source as material is removed from the transport stream. This is supported by estimates of global depositional fluxes (Table 5.1) that illustrate a decrease along the transport path. The rate of attenuation and the resulting sedimentation pattern on the watershed scale is expected to be dependent on the specific characteristics of the system. To our knowledge, there are no estimates of OC deposition in the three categories outlined originally by Meade et al. (1990) from within a single watershed to permit a direct comparison among them.

Eroded CZ OC is not a conservative entity. As OC moves through a sedimentary system, portions may be oxidized or modified either during transport or when in depositional rest (Blair et al. 2004; Doetterl et al. 2016). New primary and secondary production can also overprint or replace the original OC, therefore the OC deposited is not the same OC that was eroded. We identify two key research questions: (1) Is soil erosion a net source or sink of C to the atmosphere, and (2) what happens to the C in eroded soil as it is transported and stored. In this study we begin to address both questions by attempting to track material as it moves through different traps within a single watershed.

The first objective of this study was to evaluate the inventories of eroded OC in the three general categories of sediment traps outlined by Meade et al. (1990) within the same watershed. We hypothesize that OC accumulation attenuates along the flow

path and that the bulk of the material is retained within the watershed. To test those hypotheses, a preliminary assessment is provided of the post-European settlement (~1850) depositional OC fluxes in downslope depressions, valley floodplain alluvium (designated as post-settlement alluvium or PSA, Grimley et al. 2017), and lacustrine reservoir sediments of the Upper Sangamon River Basin (USRB). This river basin is dominated by agricultural land use and is the location of the Intensively Managed Landscape Critical Zone Observatory (IML-CZO).

The second objective was to determine to what extent multiple sources of OC might be mixed with, or replace the original eroded OC. We hypothesize that a significant portion of the deposited OC is not derived solely from agricultural fields but also includes material from local primary and secondary production. Corn and soybean rotations are the primary agricultural activities in the USRB watershed; thus, the C4 plant carbon isotopic signature of the corn can be used as a tracer for eroded soil C throughout the system. Both carbon isotopic and OC biomarker measurements are used to distinguish between original row crop C and other sources such as local primary production at the depositional sites.

#### 5.1.1 Field Site

The Sangamon River feeds into the Illinois River within the Upper Mississippi River Basin (Fig. 5.1). The 2400-km² USRB terminates at the reservoir, Lake Decatur. The watershed drains a glaciated low-relief terrain with a mean slope <1% (Keefer et al. 2010). The USRB region was last glaciated about 25,000 to 21,000 years before present (Grimley et al. 2016a). Glacial sediments in uplands are typically covered by about 1 m of loess that contain mostly poorly- to moderately-drained Mollisol or Alfisol profiles (Mount 1982; Fehrenbacher et al. 1986). Alfisols and better drained soils are more common within about 1 km of the Sangamon River valley, with Mollisols otherwise dominant on uplands in the watershed. Typical soil series in the watershed include the poorly drained Drummer and Sable (Typic Endoaquolls) silty clay loams and the somewhat poorly drained Flanagan and Ipava (Aquic Argiudolls) silt loams. These soils have a high water holding capacity and relatively high organic matter content (Mount 1982; Fehrenbacher et al. 1986; Martin 1991).

The USRB watershed is in the humid, continental, climate region, typical for central Illinois. Mean annual temperature is 11 °C. Mean annual precipitation is about 1000 mm and distributed uniformly throughout the year. Spring and autumn storms that occur during periods of bare ground are particularly effective in mobilizing surface soils (Wilson et al. 2018).

Corn and soybean row crop agriculture cover over 80% of the watershed (Keefer et al. 2010). Developed urban areas cover 12% of the watershed, with grasslands and forests over 5%. Grassed and forested riparian buffers line the lower reaches of main stem of the Upper Sangamon River. The accumulation of large woody debris is prevalent in these lower reaches.

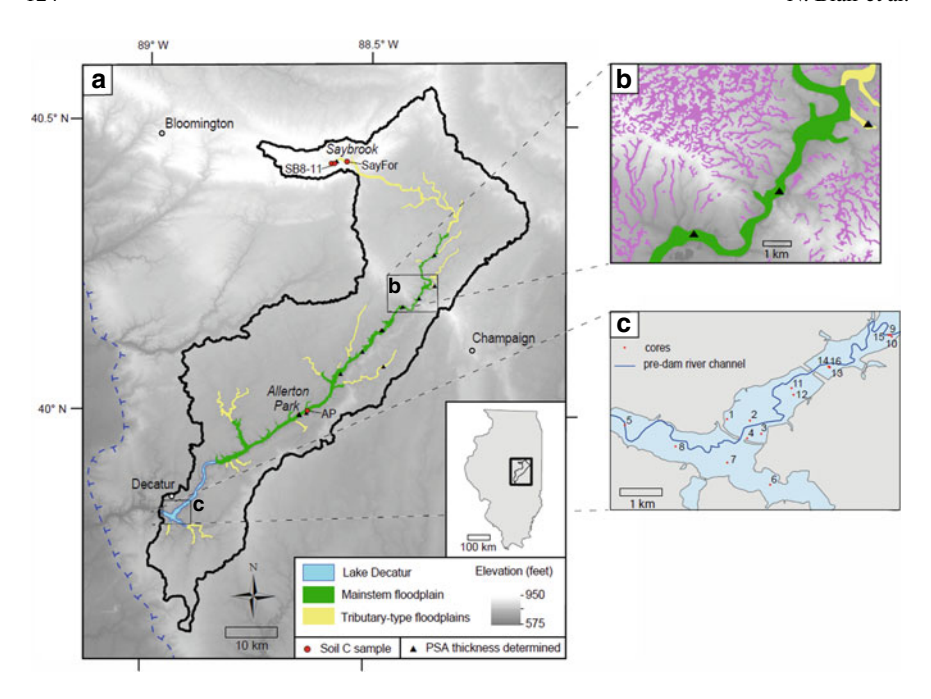


**Fig. 5.1 a** Location and surface topography (from 10 m resolution digital elevation map) of the Upper Sangamon River Basin (black outline), in east-central Illinois, within the Upper Mississippi River Basin. The mainstem (>300 m width) Sangamon River valley floodplain is highlighted in green, with tributary valley type floodplains highlighted in yellow. The dashed blue line shows the southwestern limit of glaciers during the last glacial maximum (~24 ka). Black triangles show sites with post-settlement alluvium thickness estimated from magnetic fly ash occurrence. Red dots show sampled sites for soil organic carbon. **b** Interconnected lowlands and depressions (highlighted purple) in the vicinity of Mahomet, Illinois. The Champaign Moraine extends across this area from northwest to southeast. **c** Location of coring sites in Lake Decatur with respect to the pre-dam (pre-1922) Sangamon River channel

Lake Decatur was created by the damming of the Upper Sangamon in 1922 (Fitz-patrick et al. 1987). As the result of intensive agriculture, the approximately 12 km² lake filled with sediment rapidly, necessitating frequent sediment inventories, a raising of the spillway to increase lake volume, and multiple dredging projects (Blair et al. 2018). Concerns about deteriorating water quality as a result of agriculturally-derived N-inputs initiated water column monitoring in 1967 (Borah et al. 2002). Coring of the last non-dredged segment of the lake in the lower half of the system has provided a well-constrained sedimentary record of the changes in biogeochemical fluxes within the upstream watershed through periods of dramatic climate change (e.g. major droughts) and expansion of agriculture (Blair et al. 2018).

#### 5.2 Methods

### 5.2.1 Estimates of Post-settlement Sediment Accumulation

European settlement, post-1850 in mid-North America, notably accelerated erosion and alluvial sedimentation compared to prior rates during the Holocene (Grimley et al. 2017 and references within). We have thus focused on the post-1850 settlement period when estimating inventories of OC in the major depositional sinks. This was done first by estimating of post-settlement sediment volumes and masses three depositional environments within the USRB: (1) closed basins and depressions, (2) floodplains, and (3) Lake Decatur.

The areal extent of the closed basins and depressions was estimated from the mapped occurrence of poorly drained soils in the URSB, which include mainly Drummer and Sable soil series, but also Ashkum, Elpaso (both Typic Endoaquolls), and Bryce (Vertic Endoaquoll) soil series (NRCS 2019). These soils types, comprising about 40% of the land area in the USRB (Fig. 5.1), occupy areas of former wetlands (Suloway and Hubbell 1994) that are now drained for agricultural purposes. The thickness of post-settlement accumulation in basins and depressions was estimated from prior studies in Illinois and Indiana that utilize the first occurrence of magnetic fly ash from coal combustion as a late nineteenth century marker (Hussain et al. 1998; Olson et al. 2013), or the presence of buried pre-settlement paleosol (Norton 1986).

The volume of post-settlement alluvium (PSA) in floodplains of the Upper Sangamon River Basin was estimated by assessing mean PSA thickness along both main Sangamon River valley and its tributary segments, and the measuring aerial extent of these floodplain types. Assessing the aerial extent of modern floodplains in the USRB was guided by prior statewide mapping (Lineback 1979), detailed surficial geologic mapping (Grimley et al. 2016b; Stumpf 2018), county soil survey maps (Mount 1982; Martin 1991), and digital elevation maps from the National Elevation Dataset (1/3 arc second resolution (~10 m) http://nationalmap.gov/elevation.html). Floodplains of the main Sangamon River valley and significant tributaries (e.g., Camp Creek, Friends Creek, Goose Creek, Big Ditch valleys), were digitized at ~1;100,000 scale in ESRI ArcMap 10.5.1. Small tributary valleys, <100 m wide, were not digitized because, with <40 cm thick PSA, their contribution to total PSA volume in the USRB is relatively insignificant. The main stem Sangamon River downstream of Fisher, Illinois, occupies a broad valley, likely carved by glacial meltwater, and incised 5-10 m below the surrounding upland surface. There is a marked change in slope between the Sangamon River floodplain and the valley wall, allowing for unambiguous mapping of the floodplain (Grimley et al. 2016b; Stumpf 2018). The outlines of tributary valleys were also relatively easily mapped.

PSA thickness was determined by the occurrence of magnetic fly ash in vertically sampled profiles or cores (Grimley et al. 2017). Based on an analysis of 17 localities, PSA thickness was found to be linearly related to valley width (Grimley et al. 2017); similar relationships have also been noted for small- to moderate-size valleys

Process	Flux (Pg C/yr)	% of C eroded <sup>e</sup>	
Water erosion <sup>a, b</sup>	4.0-6.0	_	Transport ↓
Colluvium/alluvium deposition <sup>a</sup>	2.8-4.2	70	
Reservoir and lake burial <sup>c, d</sup>	0.19-0.69	9	
Export to ocean <sup>c, d</sup>	0.3-0.5	8	
Ocean burial <sup>d</sup>	0.08-0.15	2	

Table 5.1 Global organic C erosional and depositional fluxes

in Wisconsin (Lecce 1997) and southern Minnesota (Beach 1994). The USRB flood-plain areas were separated into two categories (Fig. 5.1): (1) main stem Sangamon River valley (>400 m valley width) and (2) tributary valley and upper reaches (100–400 m valley width). Based on relationships determined by Grimley et al. (2017), valley widths >400 m have a typical PSA thickness of 70 cm, whereas valley widths of 100–400 m have a typical PSA thickness of 50 cm. These PSA thicknesses were assigned to the two mapped valley types and used for the final calculations of PSA volume and mass in the USRB (Table 5.2). The total volume of PSA in the USRB (discluding upland depressions) was then calculated by multiplying the area of both floodplain types by an appropriate PSA thickness, and then adding both volumes together.

In Lake Decatur, sediment accumulation was estimated from a combination of historic sediment surveys, identification of temporal markers in cores, and <sup>210</sup>Pb, <sup>137</sup>Cs radiochemistry (Fitzpatrick et al. 1987; Blair et al. 2018). Lakebed coring proceeded along and cross-channel to delineate the range of sediment column thicknesses. Reservoir sediment volume was determined using an areal-average accumulation rate integrated over the period of 1922–2015 (Blair et al. 2018).

# 5.2.2 Organic Carbon Concentrations and C-Isotopic Compositions

Organic matter concentrations for the closed basin/depression soils in the USRB were obtained for the Drummer-Sable series from the National Cooperative Soil Survey (NRCS 2019). Organic matter values were converted to organic C (as percent of sediment dry weight) using an average C content of 50% (Pribyl 2010). Organic C concentrations and  $^{13}\text{C}/^{12}\text{C}$  ratios ( $\delta^{13}\text{C}$ ) were previously reported by us on individual samples collected from the excavations of the banks along the Upper Sangamon and cores recovered from Lake Decatur (Fig. 5.1; Blair et al. 2018). Soil samples SB8-11

<sup>&</sup>lt;sup>a</sup>Lal (2003)

<sup>&</sup>lt;sup>b</sup>Doetterl et al. (2016)

<sup>&</sup>lt;sup>c</sup>Cole et al. (2007)

<sup>&</sup>lt;sup>d</sup>Blair et al. (2018) and citations within

<sup>&</sup>lt;sup>e</sup>Calculated using mean values of ranges

Process/location	Total sediment (Tg) <sup>a</sup>	Gg C/yr <sup>b</sup>	% of total OC <sup>c</sup>
Upland loss	$221 \pm 79^{d}$	$42.8 \pm 11.6$	
Depressions/closed basins	$134 \pm 55$	19 ± 14	59
Tributary floodplains	29 ± 9	$4.0 \pm 3$	13
Main stem floodplains	49 ± 12	$6.8 \pm 5.1$	21
Lake Decatur	$6.5 \pm 2.2$	$1.8 \pm 0.4$	6
Export from Lake Decatur	$2.2 \pm 0.7$	$0.58 \pm 0.12$	2
Total deposited	221 ± 79	$31.6 \pm 15.4$	
Potential oxidative loss <sup>e</sup>		$11.2 \pm 27$	26

Table 5.2 Post-settlement sediment and OC erosion and accumulation in the Upper Sangamon River Basin

and SayFor were collected in the Saybrook upland area (Fig. 5.1). Additional samples were obtained from the lowland floodplain portion of the watershed (Allerton Park, AP). The SB8-11 and AP samples were from exposed banks that were scraped to remove approximately 1 cm of surface material to access fresh material. Samples were collected from just below the litter layer down almost to stream level. The alluvial soils exposed in the sampled streambanks are classified as Sawmill silty clay loam (Cumulic Endoaquolls). SB11 was from the same location as cores FA-4a,b in Grimley et al. (2017). Holocene alluvium represents 91–97 cm of deposition at that site, of which the upper 40–42 cm was characterized as post-European settlement (post-1870). The AP samples were collected near the studied bank exposure FA-5, where PSA was found to be 70 cm thick (Grimley et al. 2017). The total Holocene alluvial deposition in the Sangamon Valley at Allerton Park is approximately 550 cm.

The SayFor surface-soil (0–5 cm) was collected from a forested area within a transition zone between the Sawmill and Lawson Aquic Cumulic Hapludolls soil types. "SB11 corn" was a surface sample (0–5 cm) from a field planted in corn at the time of sampling at the border of the Sawmill and the Warsaw loam (Mollisol, Typic Endoaquolls). All soils were stored frozen until analysis.

Lakebed sediments were collected using a gravity corer in May 2014 and a vibracorer in June 2015, both equipped with polycarbonate tubing. Station locations and ID numbers are shown in Fig. 5.1 and described in Blair et al. (2018). The cores were extruded and subsampled in 5 cm intervals with 12 mL cut-off plastic syringes. Two cut-off syringes were used to fill 15 mL centrifuge tubes. The sediment was isolated from porewater by centrifugation (4000 rpm for 30 min). The sediment recovered from the centrifugation were archived frozen until further processing and analysis.

<sup>&</sup>lt;sup>a</sup>Total post-settlement sediment accumulated for 145 years on the landscape or 93 years in the reservoir. The export term is for the lifetime of the reservoir

<sup>&</sup>lt;sup>b</sup>Mean accumulation of OC between high-low estimates normalized to the lifetime of the feature (145 or 93 years). Uncertainties represent the high-low ranges of the estimates

<sup>&</sup>lt;sup>c</sup>Computed from the mean Gg C/yr estimates for deposition

<sup>&</sup>lt;sup>d</sup>Upland erosive loss of soil is assumed to be equal to the total deposited sediment

<sup>&</sup>lt;sup>e</sup>Oxidative loss = Upland loss - total deposited

All sediment samples were lyophilized and ground to a fine powder. Samples were treated with either gaseous HCl (for soils) or aqueous 2N HCl (lake sediments) to remove carbonates. Carbonate removal was verified via transflectance FTIR (Cui et al. 2016) using a Bruker Tensor 37 FTIR [NIR/MIR] equipped with a Hyperion microscope and MCT detectors by monitoring an absorbance peak at 2513 cm<sup>-1</sup>.

The decarbonated soils and sediment samples were analyzed for OC concentrations and stable isotopic compositions using a Costech Elemental Analyzer-Conflo IV interface-Thermo Delta V Plus isotope ratio mass spectrometer (IRMS) combination. Individual analyses of the various depth intervals from bank exposures and lake cores were not replicated in most cases. Sample sizes (>100  $\mu g$ ) were above the lower limit for reliable analyses (40  $\mu g$ ). Typical analytical precisions were  $\pm 0.1\%$  and  $\pm 0.2\%$  for %C and  $\delta^{13}C$  measurements respectively as determined by periodic sample and reference material replications. Samples within a group (bank, lakebed) were pooled to create pseudo-replicates and provide a measure of breadth of values within each group.

#### 5.2.3 Biomarkers

Biomarker (cellulose, lignin phenols, and long-chained lipids) measurements, previously unreported, were performed on Lake Decatur sediments from a single core (9, Fig. 5.1) using a broad spectrum analysis employing tetramethylammonium hydroxide (TMAH) thermochemolysis (del Rio et al. 1998). The core was chosen because of its well-constrained geochronology that allows us to specify the time of sediment deposition to within ~5 years over a 55 year record (Blair et al. 2018). The TMAH reagent methylates many O-containing functional groups (esters, ethers, carboxylate acids, alcohols) to form methyl esters and ethers (del Rio et al. 1998; Filley et al. 2006). The reaction was done on ~1 mg of OC at 300 °C for 30 s on-line using a CDS pyrolysis unit coupled to a Thermo Trace GC—DSQ II mass spectrometer. Detection limits were ~0.1 mg C, the exact value being dependent on the molecular composition of the sample. The total ion current response of each compound peak was normalized to an internal standard, methyl-D3 pentadecanoic acid methyl ester, and the resulting values then further normalized to the organic C content of the sample. Because of uncertainties concerning potential matrix effects on the TMAH reaction yield and the absolute concentrations, C-normalized concentrations are reported in relative abundance compared to the maximum observed concentration of a compound across all samples of the same matrix. The analytical precision was <0.1 on the relative concentration scale. These relative values were summed for the lignin phenols to create the  $\sum$  lignin index (Fig. 5.4). All compounds were identified using a combination of NIST and in-house mass spectral libraries and published spectra (Fabbri and Helleur 1999). For NIST identified compounds, a reverse squared index (RSI) value of 800+ constituted a positive identification.

#### **5.3** Results and Discussion

#### 5.3.1 Sediment and OC Inventories

The masses of post-settlement accumulation in downslope basins and depressions, valley floodplains and Lake Decatur sediments, as determined from volumes, are summarized in Table 5.2. Accumulation thicknesses were highly variable illustrating the topographic patchiness of these features. Thickness determination was also complicated by the effect of mixing processes on vertical tracer distributions (Olson et al. 2013). The interpretation of data from western Illinois and Indiana have suggested that post-settlement accumulation thicknesses in depressions and at the base of hillslopes range from ~6 to ~25 cm (Norton 1986; Hussain et al. 1998; Olson et al. 2013). We use a nominal conservative value of  $10 \pm 5$  cm. We do not have tracer studies of the downslope environments in the USRB currently, however visual observations of the soils suggest this is a reasonable estimate. Coupled with the areal estimate of  $960 \times 10^6$  m², the computed volume of the downslope sediment accumulation is  $96 (\pm 48) \times 10^6$  m³.

PSA thicknesses within floodplains in the USRB ranged from 25 to 95 cm based on fly ash occurrence (Grimley et al. 2017). We used a mean value of  $70 \pm 20$  cm for the mainstem valley deposits and  $50 \pm 20$  cm for the tributary valley. Estimated volumes of the valley PSA are  $20~(\pm 7.4) \times 10^6~\text{m}^3$  and  $35~(\pm 10) \times 10^6~\text{m}^3$  for the tributary and mainstem respectively.

Sediment accumulation has varied with time and location in Lake Decatur. Initially, sediment accumulation rates tended to be highest in the original river channel after dam emplacement (Blair et al. 2018). Eventually rates began to even out as the channels infilled. Measured rates ranged from 0.8 to 2 cm/yr, with a lake-wide average of 1.5  $\pm$  0.5 cm/yr for the nearly 90 year history of the reservoir (Blair et al. 2018). The total volume of sediment is estimated to be 17  $(\pm 5.6) \times 10^6~\text{m}^3$ .

Particulate organic carbon (POC) concentrations were measured on the PSA from bank deposits along the Sangamon and in Lake Decatur (Fig. 5.2). Banks deposits had concentrations of ~1–3.6% at the surface in the 0–5 cm depth interval. The lowest concentration was from bare soil in a corn field, the highest in a forest soil (Blair et al. 2018). Concentrations decreased with depth to values <1% in the lower solum as is typically seen in soil profiles. The concentration gradient is due primarily to the surface inputs from vegetation followed by degradative losses with depth of burial. A concentration of  $1.6 \pm 0.8\%$ , based on mean values for PSA samples, was used to determine the quantity of post-settlement POC stored in the floodplains. Closed basin/depression POC concentrations were estimated to be  $2.5 \pm 0.5\%$  based on data from the Web Soil Survey (NRCS 2019). The volumes of stored sediment were converted to masses using a dry bulk density of 1400 kg/m³. Mean quantities of OC sequestered in the depressions/closed basins, tributary and main stem floodplains were 2.7, 0.57, and 0.98 Tg respectively.

Lake Decatur sediments had POC contents of ~0.5–3% with most values being >1% (Fig. 5.3). Concentrations generally decreased with depth into the lakebed.

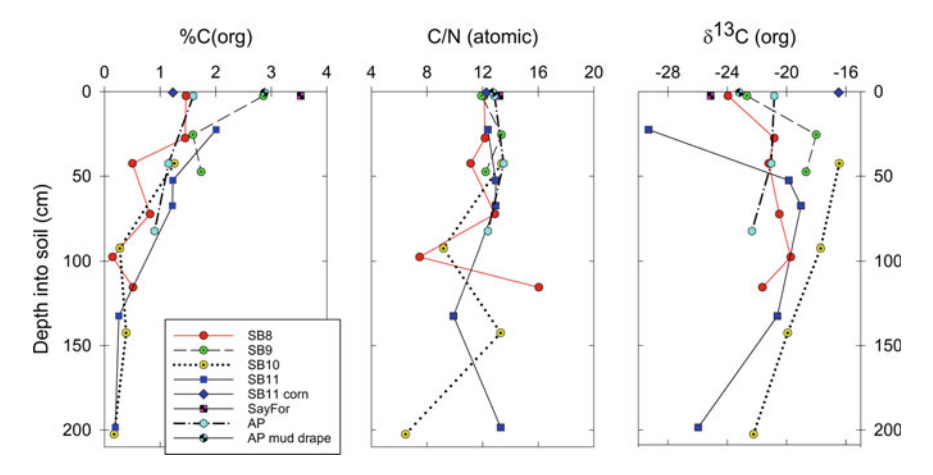


Fig. 5.2 Particulate organic C contents (as %C dry weight), organic C/total N (C/N on a per atom basis), and  $\delta^{13}$ C of particulate OC as a function of depth from surface at multiple river bank exposures. PSA depths are ~40–70 cm

While some of the attenuation is due to degradative processes, the largest changes were associated with gradients in sediment grain size that accompanied a transition from original valley floor coarse-grained sediments to accumulating lake mud (Blair et al. 2018). We used a mean POC content of  $2.2 \pm 0.7\%$  and a bulk density of 390 kg dry sediment/m³ wet sediment to determine the quantity of C sequestered in the lake (0.16~Tg). Insofar as the reservoir is approximately 75% efficient in its retention of sediment (Fitzpatrick et al. 1987), we estimate that 0.05~Tg C were exported past the dam.

The terrestrial and lacustrine accumulations of sediment and OC are products integrated over different time frames. Post-settlement accumulation on the landscape has occurred for approximately 145 years following extensive clearing of native vegetation for agricultural purposes (Grimley et al. 2017). Accumulations in Lake Decatur had occurred for 93 years prior to sample collection. Average annual OC accumulation rates have been computed to permit comparisons of the pools of sequestered material (Table 5.2). Historically, the depressions/closed basin have trapped ~59% of the total OC on a per annual basis, whereas floodplains accumulated ~34%, and Lake Decatur has sequestered 6%, allowing ~2% to escape the system. Total accumulation on the landscape as opposed to going to or past Lake Decatur was 92%. The large pool of trapped carbon in depressions and closed basins is consistent with sediment fingerprinting studies in sub-basins of the USRB that indicate that the majority of suspended sediment carried by streams is derived from near-channel sources rather than being removed from upland agricultural fields (Neal and Anders 2015; Yu and Rhoads 2018). In essence, the sediment is trapped and slowly released over time.

The tendency for sediment to be trapped on the landscape above the channel network is expected to vary considerably with topography. The USRB has been strongly impacted by recent glaciation which disrupted the pre-glacial stream

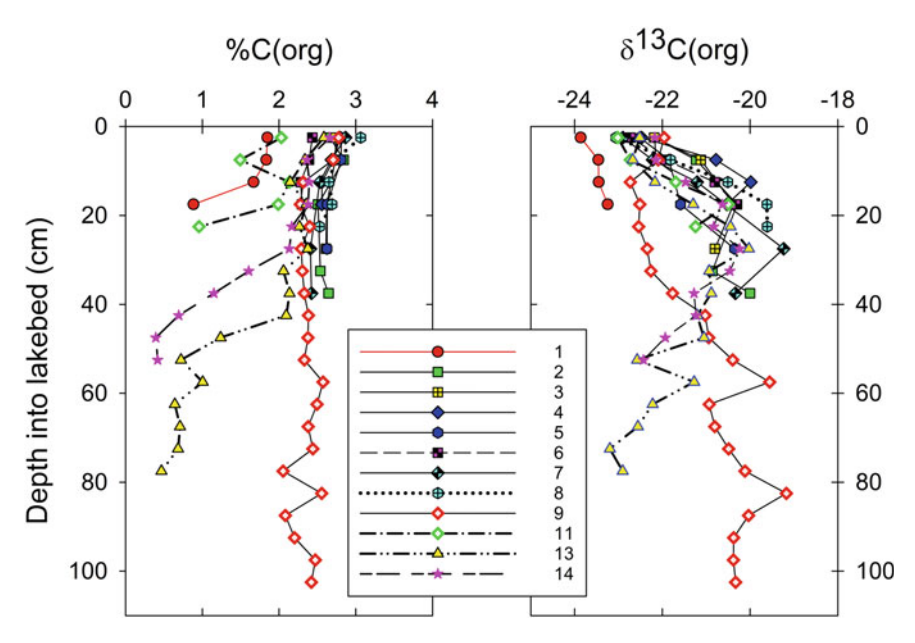


Fig. 5.3 Particulate organic C contents (as %C dry weight) and  $\delta^{13}$ C of particulate OC in Lake Decatur sediments as a function of depth into lakebed

network, leaving large portions of the land surface disconnected from external drainage systems (Anders et al. 2018; Lai and Anders 2018). The resulting closed depressions and swales are effective traps of sediment and, the poor drainage and topographic position of these areas allowed for the accumulation and preservation of high concentrations of organic carbon. While large portions of the Upper Mississippi drainage basin have experienced glaciation, the time since most recent glaciation varies from >500,000 to ~12,000 years (Anders et al. 2018), leading to large differences in extent of post-glacial integration of stream networks to drain the uplands (e.g., Ruhe 1952). The maturity of drainage networks, along with the glacial geomorphology, influences the distribution of sedimentation and trapping efficiency of the uplands. The recent glaciation and low relief of the USRB are factors that have led to considerable storage of sediment in upland depressions. In contrast, in the unglaciated Driftless Area of Wisconsin, sediment trapping by the landscape in the extensively studied Coons Creek watershed, is attributed primarily to floodplain aggradation with only ~10% of sediment exported from the watershed (Trimble 2009).

The Mississippi River Basin, which includes the USRB and Coons Creek watersheds, constitutes  $\sim$ 40% of the conterminous U.S. and retains  $\sim$ 90% of the eroded soil and its C (Smith et al. 2005). Deposition was nearly equally distributed between floodplains and impoundments based on the sediment budget model employed (Smith et al. 2005). A survey of sediment budgets from within the conterminous U.S. suggests that reservoirs capture  $\sim$ 48% of eroded soils on average, with a range of  $\sim$ 2 to >100% (Smith et al. 2001). Multiple factors no doubt influence the importance of reservoirs

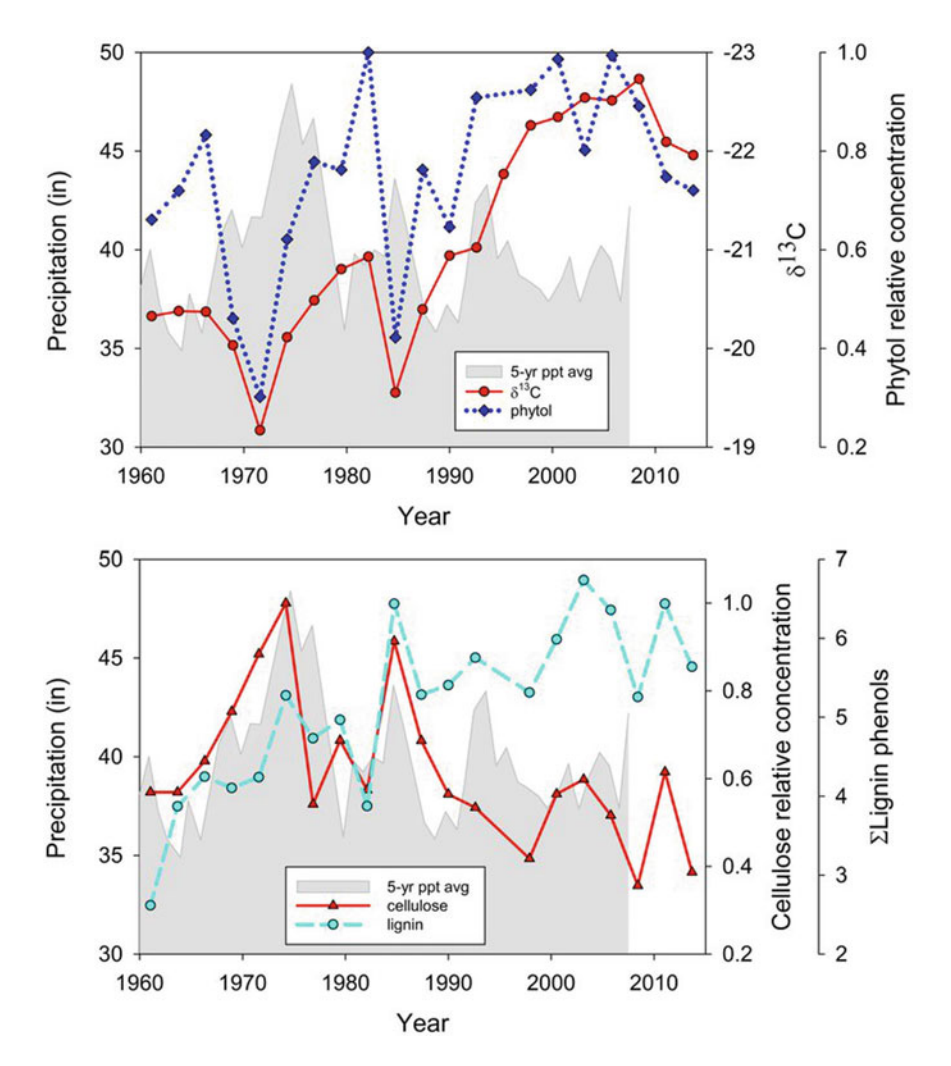


Fig. 5.4 Biomarker and isotopic analyses of Lake Decatur core 9 (Figs. 5.1 and 5.3). Top panel—Particulate OC  $\delta^{13}$ C and phytol (relative concentration) as functions of approximate time of deposition based on the age model for the core (Blair et al. 2018). Bottom panel—Cellulose proxy and the sum of lignin phenols as a function of approximate time of deposition. Included in both panels is the 5-year rolling average of annual precipitation at Monticello station (in inches) as a function of actual year

with dam placement location being one of them. Reservoirs in river headwaters would be in a position to starve downstream floodplains as an example (Downs et al. 2018). In short, while there is general agreement that eroded soil and its C tends to stay within the system, exactly where it accumulates will vary as a function of watershed characteristics, including topography, geomorphic history, and the presence and location of lacustrine environments.

The question remains whether the soil OC erosion creates a net source or sink of atmospheric C on the watershed scale. We can constrain the answer somewhat by assuming that all the eroded soil has been accounted for in the various depositional traps (221  $\pm$  79 Tg, Table 5.2). This is equivalent to an average eroded soil thickness of ~13 cm when placed on the upland (non-depositional) portion of the watershed and an average erosion rate of 0.9 mm/yr over the 145 years. This is well within the range noted for agriculturally enhanced erosion rates (Montgomery 2007). We must also assume an organic C content of the original surface soil. This is problematic because soil OC contents are typically reported on multi-centimeter not millimeter scales. Using available data for mid-Illinois upland forests and restored prairie surface soils (0–15 cm), we estimate a C-concentration of  $35.7 \pm 9.7$  kg/m<sup>3</sup> in the original soils (Olson et al. 2012; Tsai et al. 2014; Li et al. 2020; Olson and Gennadiev 2020). The total OC inventory that was projected to have been lost to the combination of oxidation and erosion is thus  $6.2 \pm 1.7$  Tg, at a rate of  $42.8 \pm 11.6$  Gg C/yr (Table 5.2). This is likely an underestimate because of the thick soil intervals employed for the measurements. When compared to the depositional flux, it is estimated that the oxidation loss rate was  $11 \pm 27$  Gg C/yr. In other words, this approach alone is not sensitive enough to resolve the source or sink question. There are two primary sources of uncertainty that ultimately must be resolved if one is to move from a plot to watershed scale. The first is developing a better understanding of PSA thicknesses in the shallow depressions. The second is constraining OC contents of surface soils over a wide range of environments within the watershed. Neither will be accomplished with more point measurements alone and will likely require some combination of remote sensing and modeling to extrapolate over large areas. A 3-D biogeochemical model that couples soil erosion and deposition, OC transformations and landscape evolution successfully emulated landscape OC distributions in the much smaller Clear Creek watershed (Yan et al. 2019). It provides an example of a future approach to this problem.

## 5.3.2 Organic C Sources and Composition

Carbon stable isotopes ( $^{13}$ C/ $^{12}$ C) provide a tracer for row crop OC because of corn's C4 photosynthetic pathway. C4 plants are enriched in  $^{13}$ C ( $8^{13}$ C  $\sim$ -10 to -13%) relative to more common C3 vegetation ( $8^{13}$ C  $\sim$ -25 to -35%) (O'Leary 1981; Farquhar 1983; Farquhar et al. 1989). In addition to corn, which has dominated the landscape in the USRB for the last century, other C4 plants found in this area are some prairie grasses (e.g. Big Bluestem; Teeri and Stowe 1976). Surface soil OC  $8^{13}$ C values were -16.5% for the SB11 cornfield sample and -16.5 to -19.5% for row crop fields in the IML-CZO sister site, Clear Creek, Iowa (Hou et al. 2018). These values reflect a mixture of corn-soybean inputs. The same  $^{13}$ C-enrichment of particulate OC has been observed in the suspended load of the Sangamon River during peak discharge (maximum observed  $8^{13}$ C = -19.5%), signaling row crop soil inputs during storm events (Blair et al. 2018).

δ<sup>13</sup>C measurements of bank exposures reveal a record of changing OC sources (Fig. 5.2). Peak <sup>13</sup>C-enrichment is observed in multiple exposures between the depths ~25 and 75 cm which we interpret as the accumulation of PSA with a dominant POC source derived from row crops. Above those depths, the <sup>13</sup>C-enrichment decreases and  $\delta^{13}$ C values trend to more C3-plant compositions. With the exception of the Saybrook corn field sample (SB11 corn), all the sampled locations are currently vegetated with C3 plants (pasture grasses, trees), thus the reversal of the  ${}^{13}C/{}^{12}C$  ratios are likely due to present day local inputs overprinting the row crop signature. The one exception to these observations is the Allerton Park (AP) floodplain exposure. A pronounced subsurface <sup>13</sup>C-enriched peak is not observed. The site is a second growth forest that has been protected from agricultural land use (Wang et al. 2008), thus a change from C3 to mainly C4 and back to C3 vegetation has not occurred. Even so, the AP  $\delta^{13}$ C values (mean  $-21.4 \pm 0.8\%$ ) fall between the C3 and C4 plant endmember values, which must reflect alluvial input of row crop C to the site. We infer that the local forest OC inputs provide a partial but incomplete overprinting of the row crop signal. An isotopic mass balance calculation to determine the relative proportions of row crop and other OC sources would be highly uncertain because the  $\delta^{13}$ C values of the various endmembers are poorly constrained, as are potential transport and diagenetic isotope effects. Even so, if we assume a mixing of two sources, row crops ( $-18 \pm 1.5\%$ , Hou et al. 2018) and non-row crop C3 vegetation  $(-30 \pm 5\%)$ , with no subsequent fractionations approximately 72 ± 4% (mean + S.E.) of the floodplain OC can be attributed to row crop soils.

The overprinting process is not the product of simply mixing plant sources. Vascular plants display C/N ratios >20 because of their high lignocellulose content, whereas other sources of OC, including non-vascular plants and microbes, have values in the range of 6–12 (Tremblay and Benner 2006). C/N ratios of the upper meter of the bank exposures were 10–14 (Fig. 5.2). A significant portion of the bank exposure PSA OC has the characteristic of having been microbially recycled and blended (Hedges and Oades 1997; Tremblay and Benner 2006). The heterotrophic reprocessing of the soil C may also cause a potential several per mil <sup>13</sup>C-enrichment thus mimicking small additions of C4 material (Ehleringer et al. 2000).

The sources of OC in Lake Decatur sediments have evolved over the lifetime of the reservoir.  $\delta^{13}$ C values at the base of cores that intercepted the original valley floor were  $\sim 22\%$ , a value midway between C3-C4 plant signatures (Fig. 5.3). While this value might reflect original plant inputs from circa 1922, it could also be due to the mixing down of row crop inputs from later periods during storm events in shallow areas of the lake (Blair et al. 2018). The  $\delta^{13}$ C values become more positive moving upcore (and forward in time) reflecting either increasing inputs of row crop OC and/or decreasing mixing with valley floor sources (Blair et al. 2018). The isotopic trend reverses further upcore ( $\sim$ 15–40 cm in most cores), and at a time estimated to be in the 1970s based on our age models (Blair et al. 2018). We hypothesize that the reversal is due to eutrophication of the lake, which has been commonplace in many reservoirs during the same time period (Dietz et al. 2015). Changes in the proportion of corn production do not explain the variations (Blair et al. 2018). Multiple  $^{13}$ C-enriched (positive  $\delta^{13}$ C) peaks are seen throughout the core, the largest at 55–60 and

~85 cm in core 9. The peaks likely reflect periods of proportionately more row crop C delivery.

The TMAH thermochemolysis analysis of core 9 was used to further constrain the sources of the OC in Lake Decatur. Cellulose, the most abundant component in vascular plants (Duchesne and Larson 1989), produces multiple methylated derivatives (Fabbri and Helleur 1999). We have used one permethylated saccharinic acid derivative that is well-resolved in chromatograms as a cellulose proxy. The cellulose proxy exhibits multiple peaks, two of which align with those seen in the  $\delta^{13}$ C values at 55–60 (mid-1980s), ~85 cm (early to mid-1970s, Fig. 5.4). This is consistent with the conclusion that row crop C contributes preferentially to the peaks, and further constrains the source to be cellulose-rich, such as corn stover debris.

Characteristic methylated phenols are produced via the TMAH reaction with lignin (Clifford et al. 1995; Filley et al. 2006). The sum of the eight derivatives was used as a lignin proxy (Table 5.3). Though not as pronounced as for the cellulose indicator, peaks are also observed at the same depths or times of deposition (Fig. 5.4). This further verifies the episodic input of lignocellulose.

Phytol, a constituent of chlorophyll, was recognized by its methyl ether in this analysis. Whereas any plant will produce phytol, algae and vascular plant leaves are expected to have higher concentrations relative to total OC than vascular plant stems and roots, which will be rich in structural components such as lignocellulose. Phytol exhibits variations in abundance downcore with its lowest values corresponding with peaks in cellulose. This pattern is most consistent with a non-vascular plant photosynthetic source, i.e. algae.

The summative view derived from the biomarker and isotopic data is that soil inputs, while chronic, are not constant in flux to Lake Decatur. Logically, it is expected that large storms are responsible for the episodic input of vascular plant row crop material as well as remobilization of material stored in depressions, floodplain banks and in the lake. Individual storms are not resolvable in this geochemical record because the 5 cm sampling intervals integrate approximately 5–10 years of accumulation and this captures multiple events (Fig. 5.4). In addition, deposition in the distal half of Lake Decatur is likely not the product of a single storm event that delivers material from the original row crop source. Instead, net deposition and accumulation is expected to have a component of sediment that has experienced serial erosion—deposition cycles associated with multiple storms. Appropriately, rolling 5-yr averages of precipitation do identify potential candidate periods of increased storminess that could have expedited the erosion and delivery of row crop material to the lower portion of the lake (Fig. 5.4).

The data also indicate that row crop soils are not the sole OC inputs to the lake. Reservoir primary production is another significant source. C3 vascular plant material from riparian forests along the Sangamon River valley and pastures are other sources (Blair et al. 2018). Even though a large fraction of the sediment in Lake Decatur is likely derived from eroded agricultural surfaces, a significant fraction of the OC is not. The sediment serves as a ballast to sequester sources of OC other than the row crop soil that have become associated with it during its prior storage upstream, transport, and deposition.

**Table 5.3** TMAH derivatives identified in Lake Decatur sediments

136

Peak #	m/z <sup>a</sup>	Compound <sup>b</sup>	Source
1	129, 101, 75	Saccharinic acid	Cellulose
2	129, 101, 75	Saccharinic acid	Cellulose
3	74, 87, 186	C10 n-FA <sup>c</sup>	Lipid
4	153, 168, 125	1,2,4-trimethoxybenzene	Carbohydrate
5	166, 165, 95	Vanillin	Lignin
6	74, 87, 214	C12 n-FA	Lipid
7	165, 180, 77	Acetovanillone	Lignin
8	196, 165, 79	Vanillic acid	Lignin
9	196, 181, 110	Syringaldehyde	Lignin
10	195, 210	Acetosyringone	Lignin
11	161, 192, 133	p-Coumaric acid	Lignin
12	74, 87, 242	C14 n-FA	Lipid
13	226, 211, 195	Syringic acid	Lignin
14	148, 162, 177	Adenine	NA <sup>d</sup>
15	74, 87, 259	Methyl-D3 C15 n-FA	Internal standard
16	222, 191, 147	Ferulic acid	Lignin
17	55, 69, 236	16:1 ω7 FA	Lipid
18	74, 87, 270	C16 n-FA	Lipid
19	85, 123, 81	Phytol	Chlorophyll
20	101, 74, 326	Phytenic acid	Chlorophyll
21	74, 87, 298	C18 n-FA	Lipid
22	74, 87, 326	C20 n-FA	Lipid
23	74, 87, 354	C22 n-FA	Lipid
24	74, 87, 382	C24 n-FA	Lipid
25	74, 87, 410	C26 n-FA	Lipid

<sup>&</sup>lt;sup>a</sup>m/z = mass to charge ratio of major ions

#### 5.4 Conclusions

Inventories of post-settlement sediment and OC accumulation in downslope basins and depressions, valley floodplains and Lake Decatur sediments support the hypothesis and prevailing view that deposition of eroded materials occurs primarily near to the source and attenuates with transport distance. Approximately 90% of the accumulation can be found in basin/depression and floodplain environments and nominally 10% escapes downstream to the reservoir and beyond. Even though reservoirs have been argued to trap a major portion of eroded sediments globally (Smith et al. 2001;

<sup>&</sup>lt;sup>b</sup>Compounds are methyl ester and/or ether derivatives

<sup>&</sup>lt;sup>c</sup>Cx FA = x-carbon chain length fatty acid. Fatty acids are from extractable and bound lipids

<sup>&</sup>lt;sup>d</sup>Probable sources are nucleic acids

Syvitski et al. 2005), our results suggest that while global reservoir sediment accumulation is a significant term, the landscape itself is quantitatively more important. A similar conclusion was reached for post-Neolithic Central Europe where eroded soil OC storage on hillslopes and floodplains was several orders of magnitude greater than that in lakes and reservoirs (Hoffmann et al. 2013). However, this conclusion may be highly dependent on landscape characteristics (e.g., relief, substrate lithology, age, drainage interconnectivity, river gradients, valley widths, and vegetation cover) and reservoir characteristics. More direct comparisons of the three general depocenters in different environments are needed.

Using the distinctive  $^{13}$ C/ $^{12}$ C signature of the C4 plant crop, corn, we have traced both the transport of the row crop soil OC from field source and documented its dilution and/or partial replacement by other sources. Relatively positive  $\delta^{13}$ C values signaling row crop OC were evident in floodplain and lacustrine sediments. The C-isotopes also indicated the addition of C3 sources in both locations over the last few decades. The conversion of some cropland to riparian buffer during this time may be responsible on the floodplains, and eutrophication is the likely driver in Lake Decatur. Thus, not all the OC sequestered in the depocenters is of row crop origin even though it is mainly associated with sediment whose erosion was accelerated by agricultural activities.

OC concentrations are higher on surfaces that are in contact with new primary production (vegetation and lake primary production) but are lower in the subsurface because of diagenetic losses. This raises the possibility that overall, there is not a significant net increase in OC loading on eroded sediment when post-settlement material is considered in its entirety. Exceptions may occur when deposition is rapid, the environment is anoxic such that OC is better preserved, as occurs in the lake sediments. This is the primary reason OC concentrations attenuate less with depth in the lacustrine sediments relative to the exposed floodplain deposition.

Erosion and deposition are by nature episodic functions. The organic geochemical record in Lake Decatur has captured periods of enhanced row crop OC inputs that appear to have been associated with multi-year periods with more frequent and/or more intense storm events. This relationship between storms and OC burial goes beyond the simple rainfall-surface erosion relationship so commonly assumed (Papanicolaou et al. 2015). In agricultural settings, storms tip waterways from eutrophied reactors to transporters of OC derived from in-channel primary and secondary production, surface soils, and bank erosion (Cole et al. 2007; Blair et al. 2018). Bank erosion, which is highly dependent on discharge, may contribute up 80% of the sediment in low-gradient agricultural settings (Lamba et al. 2015). The bank OC is a complex mixture of young and aged material derived from soils developing on alluvial parent material as illustrated by our analyses (Fig. 5.2). A positive correlation between watershed sediment yield and precipitation is well established, especially for steep-sloped systems (Kao and Milliman 2008), and this is expected for OC as well. Considering the complexity of OC mixtures transported during precipitation events, it is unclear how exactly the OC composition of the OC might respond to storm intensity, however. The Lake Decatur data suggests that row crop surface erosion becomes more dominant. Future climate scenarios for the Midwest U.S. that include

more flooding (Byun et al. 2019) are predicted to facilitate the transport of eroded C further from its source. That, coupled with continued anthropogenic replumbing of the hydroscape, by channelization and tile draining, will likely significantly change the trapping efficiency of the landscape in the future.

Recognizing that the landscape of the USRB represents a low relief endmember for terrestrial environments is important for considering how the conclusions from this study could be generalized. The glacial legacy of the USRB clearly favors trapping of mobilized sediment near its source. This contrasts with Clear Creek (IA), another IML-CZO site that was glaciated during the pre-Illinois Episode (~0.5–2.4 Ma), and in which the connectivity between hillslopes and river channels is much greater (Wilson et al. 2018). We predict more similar carbon and sediment storage patterns in other forelands of continental ice sheets including, for example, the area draining to the Baltic Sea (Patton et al. 2016). We further suggest that areas underlain by loess deposits, such as the Chinese Loess Plateau, are also likely to be generally similar to our study area (Fu et al. 2017). In contrast, actively uplifting mountain belts comprise the high relief endmember of terrestrial environments, and while constituting a small portion of the land surface deliver disproportionately large fluxes of sediment to the oceans (Milliman and Syvitski 1992). Long-term storage of sediment and carbon within these landscapes is not expected (Leithold et al. 2016). Numerical landscape evolution models of these systems frequently force connectivity of water and sediment between hillslopes and channels, thus bypassing lowland storage (Bishop 2007). Despite this general assumption of rapid and complete transport, it is clear that sediment is stored within actively uplifting mountain ranges (Mishra et al. 2019) both within the uplands in colluvial hollows and at the toes of hillslopes, and in river corridors in fill terraces, landslide-dammed lakes (Mackey et al. 2011) and floodplains (Blair et al. 2010). Storage volumes relative to those eroded must be relatively small, however. Landscape morphology, lithology, climate and anthropogenic activities clearly also impact the nature, distribution, and timescale of storage of sediment and carbon in these settings (Mao et al. 2009). An important consequence of the differences between high and low relief systems concerns the nature of the OC exported from the continents to the global ocean. Particulate OC exported by small, mountainous rivers will reflect upland sources (Blair and Aller 2012). The particulate OC delivered by low gradient systems will have been extensively modified by virtue of the storage and cycling in lowland soils, thereby erasing the upland organic geochemical signature, and replacing it with that derived from the storage sites. Ocean chemistry and sedimentological records are profoundly affected (Blair and Aller 2012). Carbon storage in colluvium and alluvium is a non-negligible part of the terrestrial carbon budget (Stallard 1998) and constraining the anthropogenic influences on this storage is worthy of further study. This is especially relevant now because of the anthropogenic acceleration of alluvial sediment formation (Syvitski et al. 2005; Kemp et al. 2020).

**Acknowledgements** We thank the many IML-CZO team members who have contributed to the project in the forms of field assistance, advice, sample collection and analyses, and just good comradery. Special thanks to Laura Keefer, Thanos Papanicolaou, Chris Wilson, Lonnie Leithold,

Laurel Childress, Doug Schnoebelen, Bruce Rhoads, and the rest of team Decatur. Andrew Stumpf provided information concerning soil sampling locations and classifications as well as assistance with soil sampling. Financial support was provided by the U.S. National Science Foundation (NSF) Grant # EAR-1331906 for the Critical Zone Observatory for Intensively Managed Landscapes (IML-CZO), and EAR-2012850 for the project Network Cluster CINET: Critical Interface Network in Intensively Managed Landscapes, both multi-institutional collaborative efforts. We thank Jon Chorover and an anonymous reviewer for their helpful suggestions concerning this manuscript.

#### References

- Aller RC, Blair NE (2006) Carbon remineralization in the Amazon-Guianas tropical mobile mudbelt: a sedimentary incinerator. Cont Shelf Res 26(17–18):2241–2259. https://doi.org/10.1016/j.csr.2006.07.016
- Amundson R, Berhe AA, Hopmans JW, Olson C, Sztein AE, Sparks DL (2015) Soil and human security in the 21st century. Science 348(6235). https://doi.org/10.1126/science.1261071
- Anders AM, Bettis EA, Grimley DA, Stumpf AJ, Kumar P (2018) Impacts of quaternary history on critical zone structure and processes: examples and a conceptual model from the intensively managed landscapes critical zone observatory. Front Earth Sci 6. https://doi.org/10.3389/feart. 2018.00024
- Beach T (1994) The fate of eroded soil: sediment sinks and sediment budgets of agrarian landscapes in southern Minnesota, 1851–1988. Ann Assoc Am Geogr 84(1):5–28
- Berhe AA, Harte J, Harden JW, Torn MS (2007) The significance of the erosion-induced terrestrial carbon sink. Bioscience 57(4):337–346. https://doi.org/10.1641/b570408
- Bishop P (2007) Long-term landscape evolution: linking tectonics and surface processes. Earth Surf Proc Land 32(3):329–365. https://doi.org/10.1002/esp.1493
- Blair NE, Aller RC (2012) The fate of terrestrial organic carbon in the marine environment. In: Carlson CA, Giovannoni SJ (eds) Annual review of marine science, vol 4, pp 401–423. https://doi.org/10.1146/annurev-marine-120709-142717
- Blair NE, Leithold EL, Aller RC (2004) From bedrock to burial: the evolution of particulate organic carbon across coupled watershed-continental margin systems. Mar Chem 92(1–4):141–156. https://doi.org/10.1016/j.marchem.2004.06.023
- Blair NE, Leithold EL, Brackley H, Trustrum N, Page M, Childress L (2010) Terrestrial sources and export of particulate organic carbon in the Waipaoa sedimentary system: problems, progress and processes. Mar Geol 270(1–4):108–118. https://doi.org/10.1016/j.margeo.2009.10.016
- Blair NE, Leithold EL, Papanicolaou ANT, Wilson CG, Keefer L, Kirton E et al (2018) The C-biogeochemistry of a Midwestern USA agricultural impoundment in context: Lake Decatur in the intensively managed landscape critical zone observatory. Biogeochemistry 138(2):171–195. https://doi.org/10.1007/s10533-018-0439-9
- Borah DK, Demissie M, Keefer LL (2002) AGNPS-based assessment of the impact of BMPs on nitrate-nitrogen discharging into an Illinois water supply lake. Water Int 27(2):255–265
- Byun K, Chiu CM, Hamlet AF (2019) Effects of 21st century climate change on seasonal flow regimes and hydrologic extremes over the Midwest and Great Lakes region of the US. Sci Total Environ 650:1261–1277. https://doi.org/10.1016/j.scitotenv.2018.09.063
- Clifford DJ, Carson DM, McKinney DE, Bortiatynski JM, Hatcher PG (1995) A new rapid technique for the characterization of lignin in vascular plants—thermochemolysis with tetramethylammonium hydroxide (TMAH). Org Geochem 23(2):169–175
- Cole JJ, Prairie YT, Caraco NF, McDowell WH, Tranvik LJ, Striegl RG et al (2007) Plumbing the global carbon cycle: integrating inland waters into the terrestrial carbon budget. Ecosystems 10(1):171–184. https://doi.org/10.1007/s10021-006-9013-8

- Cui L, Butler HJ, Martin-Hirsch PL, Martin FL (2016) Aluminium foil as a potential substrate for ATR-FTIR, transflection FTIR or Raman spectrochemical analysis of biological specimens. Anal Methods 8(3):481–487. https://doi.org/10.1039/c5ay02638e
- del Rio JC, McKinney DE, Knicker H, Nanny MA, Minard RD, Hatcher PG (1998) Structural characterization of bio- and geo-macromolecules by off-line thermochemolysis with tetramethylammonium hydroxide. J Chromatogr A 823(1–2):433–448
- Dietz RD, Engstrom DR, Anderson NJ (2015) Patterns and drivers of change in organic carbon burial across a diverse landscape: insights from 116 Minnesota lakes. Global Biogeochem Cycles 29(5):708–727. https://doi.org/10.1002/2014gb004952
- Doetterl S, Berhe AA, Nadeu E, Wang ZG, Sommer M, Fiener P (2016) Erosion, deposition and soil carbon: a review of process-level controls, experimental tools and models to address C cycling in dynamic landscapes. Earth Sci Rev 154:102–122. https://doi.org/10.1016/j.earscirev.2015.12.005
- Downs PW, Dusterhoff SR, Leverich GT, Soar PJ, Napolitano MB (2018) Fluvial system dynamics derived from distributed sediment budgets: perspectives from an uncertainty-bounded application. Earth Surf Proc Land 43(6):1335–1354. https://doi.org/10.1002/esp.4319
- Duchesne LC, Larson DW (1989) Cellulose and the evolution of plant life. Bioscience 39(4):238–241. https://doi.org/10.2307/1311160
- Ehleringer JR, Buchmann N, Flanagan LB (2000) Carbon isotope ratios in belowground carbon cycle processes. Ecol Appl 10(2):412–422. https://doi.org/10.2307/2641103
- Fabbri D, Helleur R (1999) Characterization of the tetramethylammonium hydroxide thermochemolysis products of carbohydrates. J Anal Appl Pyrol 49(1–2):277–293. https://doi.org/10.1016/s0165-2370(98)00085-0
- Farquhar GD (1983) On the nature of carbon isotope discrimination in C-4 species. Aust J Plant Physiol 10(2):205–226
- Farquhar GD, Ehleringer JR, Hubick KT (1989) Carbon isotope discrimination and photosynthesis. Annu Rev Plant Physiol Plant Mol Biol 40:503–537. https://doi.org/10.1146/annurev.arplant.40. 1.503
- Fehrenbacher JB, Jansen IJ, Olson KR (1986) Loess thickness and its effect on soils in Illinois. Illinois Agric Exp Station Bull 782:1–14
- Filley TR, Nierop KGJ, Wang Y (2006) The contribution of polyhydroxyl aromatic compounds to tetramethylammonium hydroxide lignin-based proxies. Org Geochem 37(6):711–727. https://doi.org/10.1016/j.jorggeochem.2006.01.005
- Fitzpatrick WP, Bogner WC, Bhowmik NG (1987) Sedimentation and hydrologic processes in Lake Decatur and its watershed. Illinois State Water Survey, Champaign, IL
- Fu B, Wang S, Liu Y, Liu J, Liang W, Miao C (2017) Hydrogeomorphic ecosystem responses to natural and anthropogenic changes in the Loess Plateau of China. Annu Rev Earth Planet Sci 45(1):223–243. https://doi.org/10.1146/annurev-earth-063016-020552
- Grimley DA, Anders AM, Stumpf AJ (2016a) Quaternary geology of the Upper Sangamon River Basin: glacial, postglacial, and postsettlement history. In Lasemi Z, Elrick SD (eds) 1967–2016—Celebrating 50 years of geoscience in the Mid-Continent: guidebook for the 50th annual meeting of the Geological Society of America–North-Central Section: Illinois State Geological Survey, Guidebook 43, 55–96
- Grimley DA, Wang JJ, Oien RP (2016b) Surficial geology of Mahomet Quadrangle, Champaign and Piatt Counties, Illinois: Illinois State Geological Survey, USGS-STATEMAP contract report, 2 sheets, 1:24,000, report, 13 p
- Grimley DA, Anders AM, Bettis III EA, Bates BL, Wang JJ, Butler SK et al (2017) Using magnetic fly ash to identify post-settlement alluvium and its record of atmospheric pollution, central USA. Anthropocene 17:84–98. https://doi.org/10.1016/j.ancene.2017.02.001
- Harden JW, Sharpe JM, Parton WJ, Ojima DS, Fries TL, Huntington TG et al (1999) Dynamic replacement and loss of soil carbon on eroding cropland. Global Biogeochem Cycles 13(4):885–901. https://doi.org/10.1029/1999gb900061
- Hedges JI, Oades JM (1997) Comparative organic geochemistries of soils and marine sediments. Org Geochem 27(7–8):319–361

- Hoffmann T, Schlummer M, Notebaert B, Verstraeten G, Korup O (2013) Carbon burial in soil sediments from Holocene agricultural erosion, Central Europe. Global Biogeochem Cycles 27(3):828–835. https://doi.org/10.1002/gbc.20071
- Hooke RL (2000) On the history of humans as geomorphic agents. Geology 28(9):843–846. https://doi.org/10.1130/0091-7613(2000)028%3c0843:Othoha%3e2.3.Co;2
- Hou T, Berry TD, Singh S, Hughes MN, Tong Y, Thanos Papanicolaou AN et al (2018) Control of tillage disturbance on the chemistry and proportion of raindrop-liberated particles from soil aggregates. Geoderma 330:19–29. https://doi.org/10.1016/j.geoderma.2018.05.013
- Hussain I, Olson KR, Jones RL (1998) Erosion patterns on cultivated and uncultivated hillslopes determined by soil fly ash contents. Soil Sci 163(9):726–738. https://doi.org/10.1097/00010694-199809000-00006
- Kao SJ, Milliman JD (2008) Water and sediment discharge from small mountainous rivers, Taiwan: the roles of lithology, episodic events, and human activities. J Geol 116(5):431–448. https://doi. org/10.1086/590921
- Keefer L, Bauer E, Markus MM (2010) Hydrologic and nutrient monitoring of the Lake Decatur Watershed: final report 1993–2008. (ed) Illinois State Water Survey, Champaign, IL
- Kemp DB, Sadler PM, Vanacker V (2020) The human impact on North American erosion, sediment transfer, and storage in a geologic context. Nat Commun 11(1). https://doi.org/10.1038/s41467-020-19744-3
- Lai JT, Anders AM (2018) Modeled postglacial landscape evolution at the southern margin of the Laurentide Ice Sheet: hydrological connection of uplands controls the pace and style of fluvial network expansion. J Geophys Res-Earth Surf 123(5):967–984. https://doi.org/10.1029/2017jf 004509
- Lal R (2003) Soil erosion and the global carbon budget. Environ Int 29(4):437–450. https://doi.org/10.1016/s0160-4120(02)00192-7
- Lamba J, Thompson AM, Karthikeyan KG, Fitzpatrick FA (2015) Sources of fine sediment stored in agricultural lowland streams, Midwest, USA. Geomorphology 236:44–53. https://doi.org/10. 1016/j.geomorph.2015.02.001
- Lecce SA (1997) Spatial patterns of historical overbank sedimentation and floodplain evolution, Blue River, Wisconsin. Geomorphology 18(3–4): 265–277
- Leithold EL, Blair NE, Wegmann KW (2016) Source-to-sink sedimentary systems and global carbon burial: a river runs through it. Earth Sci Rev 153:30–42. https://doi.org/10.1016/j.earscirev.2015. 10.011
- Li M, Foster EJ, Le PVV, Yan Q, Stumpf A, Hou T et al (2020) A new dynamic wetness index (DWI) predicts soil moisture persistence and correlates with key indicators of surface soil geochemistry Geoderma 368. https://doi.org/10.1016/j.geoderma.2020.114239
- Lineback JA (1979) Quaternary deposits of Illinois [map]. Illinois State Geological Survey: Urbana 1:500.000
- Mackey BH, Roering JJ, Lamb MP (2011) Landslide-dammed paleolake perturbs marine sedimentation and drives genetic change in anadromous fish. Proc Natl Acad Sci USA 108(47):18905–18909. https://doi.org/10.1073/pnas.1110445108
- Mao L, Cavalli M, Comiti F, Marchi L, Lenzi MA, Arattano M (2009) Sediment transfer processes in two Alpine catchments of contrasting morphological settings. J Hydrol (Amsterdam) 364(1/2):88–98. https://doi.org/10.1016/j.jhydrol.2008.10.021
- Martin WS (1991) Soil survey of Piatt County, Illinois. U.S. Department of Agriculture and Illinois Agriculture Experiment Station
- Meade RH, Yuzyk TR, Day TJ (1990) Movement and storage of sedimeny in rivers of the United States and Canada. In: Wolman MG, Riggs HC (eds) Surface water hydrology. The Geological Society of America, Boulder, CO, pp 255–280
- Milliman JD, Meade RH (1983) World-wide delivery of river sediment to the oceans. J Geol 91(1):1–21. https://doi.org/10.1086/628741

- Milliman JD, Syvitski JPM (1992) Geomorphic tectonic control of sediment discharge to the ocean—the importance of small mountainous rivers. J Geol 100(5):525–544. https://doi.org/ 10.1086/629606
- Mishra K, Sinha R, Jain V, Nepal S, Uddin K (2019) Towards the assessment of sediment connectivity in a large Himalayan river basin. Sci Total Environ 661:251–265. https://doi.org/10.1016/j.scitotenv.2019.01.118
- Montgomery DR (2007) Soil erosion and agricultural sustainability. Proc Natl Acad Sci USA 104(33):13268–13272. https://doi.org/10.1073/pnas.0611508104
- Mount HR (1982) Soil survey of Champaign County, Illinois. (ed) U.S.D.o.A.a.I.A.E. Station. U.S. Department of Agriculture and Illinois Agriculture Experiment Station
- Neal CWM, Anders AM (2015) Suspended sediment supply dominated by bank erosion in a low-gradient agricultural watershed, Wildcat Slough, Fisher, Illinois, United States. J Soil Water Conserv 70(3):145–155. https://doi.org/10.2489/jswc.70.3.145
- Norton LD (1986) Erosion-sedimentation in an closed drainage-basin in Northwest Indiana. Soil Sci Soc Am J 50(1):209–213. https://doi.org/10.2136/sssaj1986.03615995005000010040x
- NRCS (2019) Web Soil Survey [Online]. Available: https://websoilsurvey.sc.egov.usda.gov [Accessed]
- O'Leary MH (1981) Carbon isotope fractionation in plants. Phytochemistry 20(4):553–567. https://doi.org/10.1016/0031-9422(81)85134-5
- Olson KR, Gennadiev AN (2020) Dynamics of soil organic carbon storage and erosion due to land use change (Illinois, USA). Eurasian Soil Sci 53(4):436–445. https://doi.org/10.1134/s10642293 20040122
- Olson KR, Gennadiyev AN, Kovach RG, Lang JM (2013) The use of fly ash to determine the extent of sediment transport and deposition on a nearly level Western Illinois landscape. Soil Sci 178(1):24–28. https://doi.org/10.1097/SS.0b013e318284b5cd
- Olson KR, Gennadiyev AN, Zhidkin AP, Markelov MV (2012) Impacts of land-use change, slope, and erosion on soil organic carbon retention and storage. Soil Sci 177(4):269–278. https://doi.org/10.1097/SS.0b013e318244d8d2
- Papanicolaou AN, Wacha KM, Abban BK, Wilson CG, Hatfield JL, Stanier CO et al (2015) From soilscapes to landscapes: a landscape-oriented approach to simulate soil organic carbon dynamics in intensively managed landscapes. J Geophys Res-Biogeosci 120(11):2375–2401. https://doi.org/10.1002/2015jg003078
- Patton H, Hubbard A, Andreassen K, Winsborrow M, Stroeven AP (2016) The build-up, configuration, and dynamical sensitivity of the Eurasian ice-sheet complex to Late Weichselian climatic and oceanic forcing. Quatern Sci Rev 153:97–121. https://doi.org/10.1016/j.quascirev.2016.10.009
- Pribyl DW (2010) A critical review of the conventional SOC to SOM conversion factor. Geoderma 156(3–4):75–83. https://doi.org/10.1016/j.geoderma.2010.02.003
- Ruhe RV (1952) Topographic discontinuites of the Des-Moine Lobe. Am J Sci 250(1):46–56. https://doi.org/10.2475/ajs.250.1.46
- Smith SV, Renwick WH, Buddemeier RW, Crossland CJ (2001) Budgets of soil erosion and deposition for sediments and sedimentary organic carbon across the conterminous United States. Global Biogeochem Cycles 15(3):697–707. https://doi.org/10.1029/2000gb001341
- Smith SV, Sleezer RO, Renwick WH, Buddemeier R (2005) Fates of eroded soil organic carbon: Mississippi basin case study. Ecol Appl 15(6):1929–1940. https://doi.org/10.1890/05-0073
- Stallard RF (1998) Terrestrial sedimentation and the carbon cycle: coupling weathering and erosion to carbon burial. Global Biogeochem Cycles 12(2):231–257. https://doi.org/10.1029/98gb00741
- Stumpf AJ (2018) Surficial geology of Monticello Quadrangle, Piatt County, Illinois, USGS-STATEMAP contract report, 2 sheets, 1:24,000. Illinois State Geological Survey
- Suloway L, Hubbell M (1994) Wetland resources of Illinois. An analysis and atlas. Illinois Natural History Survey. Special Publication 15, 88pp
- Syvitski JPM, Vorosmarty CJ, Kettner AJ, Green P (2005) Impact of humans on the flux of terrestrial sediment to the global coastal ocean. Science 308(5720):376–380. https://doi.org/10.1126/science.1109454

- Teeri JA, Stowe LG (1976) Climatic patterns and distribution of C4 grasses in North-America. Oecologia 23(1):1–12. https://doi.org/10.1007/bf00351210
- Tremblay L, Benner R (2006) Microbial contributions to N-immobilization and organic matter preservation in decaying plant detritus. Geochim Cosmochim Acta 70(1):133–146. https://doi.org/10.1016/j.gca.2005.08.024
- Trimble SW (2009) Fluvial processes, morphology and sediment budgets in the Coon Creek Basin, WI, USA, 1975–1993. Geomorphology 108(1–2):8–23. https://doi.org/10.1016/j.geomorph.2006.11.015
- Tsai J, David MB, Darmody RG (2014) Twenty-three-year changes in Upland and Bottomland Forest Soils of Central Illinois. Soil Sci 179(2):95–102. https://doi.org/10.1097/ss.000000000 0000043
- Van Oost K, Quine TA, Govers G, De Gryze S, Six J, Harden JW et al (2007) The impact of agricultural soil erosion on the global carbon cycle. Science 318(5850):626–629. https://doi.org/ 10.1126/science.1145724
- Wang JS, Grimley DA, Xu CG, Dawson JO (2008) Soil magnetic susceptibility reflects soil moisture regimes and the adaptability of tree species to these regimes. For Ecol Manage 255(5–6):1664–1673. https://doi.org/10.1016/j.foreco.2007.11.034
- Wang ZG, Hoffmann T, Six J, Kaplan JO, Govers G, Doetterl S, et al (2017) Human-induced erosion has offset one-third of carbon emissions from land cover change. Nat Clim Change 7(5):345-+. https://doi.org/10.1038/nclimate3263
- Wilkinson BH, McElroy BJ (2007) The impact of humans on continental erosion and sedimentation. Geol Soc Am Bull 119(1–2):140–156. https://doi.org/10.1130/b25899.1
- Wilson CG, Abban B, Keefer LL, Wacha K, Dermisis D, Giannopoulos C, et al (2018) The intensively managed landscape critical zone observatory: a scientific testbed for understanding critical zone processes in agroecosystems. Vadose Zone J 17(1). https://doi.org/10.2136/vzj2018.04.0088
- Yan QN, Le PVV, Woo DK, Hou TY, Filley T, Kumar P (2019) Three-dimensional modeling of the coevolution of landscape and soil organic carbon. Water Resour Res 55(2):1218–1241. https:// doi.org/10.1029/2018wr023634
- Yu M, Rhoads BL (2018) Floodplains as a source of fine sediment in grazed landscapes: tracing the source of suspended sediment in the headwaters of an intensively managed agricultural landscape. Geomorphology 308:278–292. https://doi.org/10.1016/j.geomorph.2018.01.022